Title

Peer influence decay and behavioral diffusion in adolescent networks: A simulation approach.

Journal

Science, 392(6797)

ISSN

0036-8075

Authors

Wang, Cheng

Butts, Carter T

Hipp, John R

et al.

Publication Date

2026-04-30

DOI

10.1126/science.aea9297

Title: Peer influence decay and behavioral diffusion in adolescent networks: a simulation approach

Authors: Cheng Wang[1]*, Carter T. Butts[2,3], John R. Hipp[2,4], Cynthia M. Lakon[5]

Affiliations:

[1]Department of Sociology. Wayne State University. Detroit, MI. USA

[2]Departments of Sociology. University of California Irvine. Irvine, CA. USA

[3]Departments of Statistics, Computer Science, and EECS. University of California Irvine. Irvine, CA. USA

[4]Departments of Criminology, Law and Society. University of California Irvine. Irvine, CA. USA

[5]Department of Health, Society, & Behavior, Joe C. Wen School of Population and Public Health. University of California. Irvine, CA. USA.

*Corresponding author. Email: chengwang@wayne.edu.

Post-print. Published in Science 392(6797): 506-511. April 30, 2026.

Abstract: How far does peer influence spread through social networks before dissipating? This study investigates the diffusion of smoking behavior in adolescent friendship networks using longitudinal data from two schools (*N*=3,154) in the National Longitudinal Study of Adolescent to Adult Health. Employing Stochastic Actor-Oriented Models, we simulate interventions targeting heavy smokers using various strategies (random, in-degree, eigenvector centrality) and coverage (10%-100%). A novel exponential decay model quantifies influence attenuation, revealing indirect peer influences, or spillover effects, up to three steps from targets. Targeting 10%-30% of central individuals maximizes smoking reductions, but gains plateau beyond 40%-50% due to network saturation. In our analyses, the denser network exhibits broader diffusion and slower decay than the larger, sparser network. This decay metric optimizes intervention design across diverse network structures.

Main Text:

Peer influence, the process by which individuals adopt behaviors, attitudes, or traits from their social peers, is a potent force shaping adolescent behavior, particularly health behaviors including cigarette smoking (*1-3*). Adolescents are uniquely susceptible because of developmental sensitivities to social norms, conformity pressures, and shared activities (*4-6*). Social networks provide pathways for influence propagation, norm reinforcement, and behavioral learning (*7, 8*). Peer effects appear across numerous health domains, including obesity, substance use, and physical activity (*1, 9-11*).

These dynamics are central to social contagion theory, which posits that behaviors spread through interpersonal connections much like viruses or innovations, cascading outward from a few key individuals through social ties (*7, 12, 13*). However, unlike pathogens, behavioral influence attenuates with distance. For example, Christakis and Fowler (*1, 14*) found that behaviors like obesity or smoking ripple through friends-of-friends, but diminish with each additional link. Social influence, unlike contagion, is bidirectional: adopters are simultaneously shaped by non-adopters, potentially dampening diffusion. Despite these insights, few studies have quantified the rate at which influence decays, how it vary across networks, or how it is shaped by concurrent turnover in tie formation and dissolution over time. Such turnover complicates estimation by shifting influence pathways as behaviors spread. Without explicit metrics of influence decay, it remains difficult to evaluate the reach and indirect benefits of behavioral interventions.

This study addresses that gap by estimating peer influence decay rates across social network distance, defined as the shortest path length between two individuals at the time of intervention, using an empirically calibrated model of network and behavioral dynamics. We analyze longitudinal data from two high schools in the National Longitudinal Study of Adolescent to Adult Health (Add Health) (*15*) and use Stochastic Actor-Oriented Models (SAOMs) (*16, 17*) to simulate the co-evolution of smoking behavior and peer relationships over time.

We implement three intervention strategies: random selection, in-degree centrality (targeting students with the most friendship nominations), and eigenvector centrality (targeting students connected to influential peers). Strategies are tested across coverage levels ranging from 10% to 100% of heavy smokers. We focus on in-degree and eigenvector centrality because these measures efficiently identify individuals with greater diffusion potential (*7, 18*). By measuring both direct and indirect effects, we introduce a scalable decay parameter (δ) that quantifies how peer influence attenuates across one, two, or three degrees of separation from the targeted students.

To our knowledge, this is the first study to estimate behavioral influence decay using empirically calibrated longitudinal simulations of dynamic adolescent networks. We also assess how network saturation when most individuals are targeted or indirectly exposed reduces the marginal returns of expanding interventions. This dual focus on decay and saturation links social contagion theory to practical network intervention design.

Methods

Add Health is a nationally representative study of over 20,000 adolescents in grades 7-12 from 132 U.S. schools, including 16 in which all students were surveyed. Because Add Health contains sensitive individual-level data, we cannot publicly share it. Researchers seeking access

must apply to the Add Health archive (https://addhealth.cpc.unc.edu) and obtain formal approval in accordance with its data use and confidentiality requirements.

We analyzed two saturated schools with sufficient sample sizes (*15*): Jefferson High (19), a rural public school in the Midwest (n = 976), and Sunshine High (9), a suburban public school in the Northeast (n = 2,178). Jefferson High exhibited higher smoking prevalence and a denser friendship network whereas Sunshine High had lower smoking rates and a more diffuse structure. This contrast enables preliminary comparisons of how network structure and school composition shape the reach and effectiveness of peer-based interventions.

Results

Network reach and intervention effects

In Jefferson High, targeting 20% of heavy smokers (54 students) generates substantial network coverage with 227-252 first-degree alters, 322-401 second-degree alters, and 171-206 third-degree alters, based on targeting strategy. Centrality-based approaches (in-degree and eigenvector centrality) consistently expanded reach by selecting students with more and well-connected peers, allowing influence to cascade via highly connected paths. Table S3 (Supplemental Material) indicates network reach across selection strategies (random selection, in-degree centrality, and eigenvector centrality) and coverage levels from 10% to 100%.

In contrast, Sunshine High had a larger, fragmented network where lower connectivity limiting diffusion across comparable path lengths. Targeting 20% of heavy smokers yielded substantially smaller reach at the first, second and third degrees than in Jefferson High. This contrast highlights the importance of network cohesion, not just network size, in shaping the scalability of peer-based interventions. Corresponding reach estimates for Sunshine High are reported in Table S4 (Supplemental Material).

Across both schools, the three-step neighborhood of targeted heavy smokers covers a substantial share of students. In Jefferson High, first-, second, and third-degree alters together span 77-93% of students; in Sunshine High, despite its more diffuse structure, three-step reach still extends to about 52%. These patterns underscore the population-level leverage of network-based interventions, whereby small, strategically targeted treatments can indirectly reach large segments of adolescents.

Direct and indirect behavioral effects

Simulations revealed that targeting central individuals, those with high in-degree or eigenvector centrality, produces the strongest behavioral change, particularly at lower coverage. To illustrate, we begin with the scenario in which 20% of heavy smokers are targeted in Jefferson High using random selection (Fig. 1A), in-degree centrality (Fig. 1B), and eigenvector centrality (Fig. 1C). Each panel reports the percentage-point change in smoking at t_3 between intervention and control simulations across four social distances: targets, first-, second, and third-degree alters.

<<<<Fig. 1 about here>>>>

Random selection yielded moderate gains: non-smoking increased by +25.1% among targets and +18.4% among alters, with effects diminishing beyond one degree. In-degree targeting achieved larger, persistent improvements, including +31.3% among targets, +35.5% among alters, and +13.9% among third-degree peers. Eigenvector targeting produced similar effects, with a +35.0% increase among targets and +16.0% among third-degree peers. These

findings confirm that centrality-based strategies amplify both direct and indirect effects, though influence attenuates with distance.

Having illustrated effects at 20% coverage in Jefferson High, we next assess outcomes across selection proportions from 10% to 100%. Figs. 2A-2C present changes in non-smoking at t_3 across the same four social distances for each strategy, with shaded bands indicating relatively tight 95% confidence intervals. Across strategies, gains are largest among targets, but in-degree and eigenvector strategies yield steeper improvements at lower coverage than random selection. For instance, at 10% coverage, alters experience a +42.8% increase in non-smoking under in-degree targeting, compared to +14.4% under random.

<<<<Fig. 2 about here>>>>

Spillover effects peak at 10%- 30% coverage and then decline, especially among second- and third-degree peers. Gains level off after 50% targeting, signaling network saturation as fewer untapped ties remain. Thus, while centrality-based targeting accelerates diffusion at lower coverage, marginal returns dissipate as coverage expands, with spillover weakening progressively by social distance. This pattern aligns with diffusion ceiling and social contagion theories, which predict slowing adoption beyond critical exposure thresholds and attenuation with relational distance (*13, 20*).

The reductions in heavy smoking shown in Figs. S1A-S1C (Supplemental Material) indicate that peer influence dissipates with distance, and intervention effectiveness diminishes as coverage expands. In Jefferson High, the first 10% of centrally targeted adolescents generate the strongest indirect effects, while both direct and indirect effects plateau beyond approximately 50% coverage, consistent with saturation of the network's most influential regions.

In Sunshine High, similar patterns emerge but with smaller effect sizes, which may be associated with its larger and more diffuse network. Fig. S2A-S2C (Supplemental Material) show that centrality-based strategies, especially eigenvector targeting, outperform random selection at 10%-40% coverage. Beyond 40%-60% coverage, gains plateau and strategy differences narrow, indicating saturation. Spillover declines sharply beyond second-degree ties, with overlapping 95% confidence intervals for second- and third-degree alters rendering distal spillover effects statistically indistinguishable. Heavy smoking reduction follows a similar pattern (Figs. S3A-S3C in Supplemental Material), consistent with constraints on peer influence in more weakly connected networks.

Network-Adjusted Population Impact (NAPI)

To evaluate which targeting strategies maximize population-wide health benefits, we introduce the Network-Adjusted Population Impact (NAPI), which measures the total reduction in smoking within three degrees of the targeted heavy smokers, normalized by the number of targets. NAPI captures both the direct effects on targets and indirect spillover to first-, second-, and third-degree alters. Formally,

$$NAPI = \frac{\Delta S}{N_{target}} = \frac{S_{int} - S_{base}}{N_{target}},$$

where S_{int} and S_{base} denote total smoking load (sum of categories 0-3) within three degrees of the targets with and without intervention, respectively, and N_{target} is the number of targets.

Applying NAPI, we find that population-level gains maximize at low-to-moderate coverage rather than full saturation. As shown in Fig. S4 (Supplemental Material), in Jefferson High both in-degree and eigenvector targeting yield the largest per-target reductions at 10-30% coverage, two to three times larger than at 60-100%, with gains declining beyond 40-50% as

networks saturate. Sunshine High shows a similar but attenuated pattern, with eigenvector targeting peaking at 10-20% and flattening after 40%. Across both networks, coverage beyond 50% generates minimal additional benefit.

These findings demonstrate that maximizing population coverage requires strategic targeting of central individuals.

Influence decay rates

The classic Friedkin-Johnsen model (*2*) suggests an exponential decline in influence with network distance; we ask whether a similar pattern emerge under our more behaviorally complex framework. To assess peer influence decay, we modeled behavioral change across degrees of separation using the exponential decay function:

$$I(d) = P \cdot I_0 \cdot e^{-\delta d}$$

where $I(d)$ is the average behavioral change at distance d, P is the targeting proportion, I_0 is the average change among directly targeted individuals ($d = 0$), and δ is the decay rate. We estimated δ using log-linear regression on simulated behavioral outcomes for distances $d = 0$ through 3, assuming multiplicative error. This specification allows δ to be interpreted directly as the rate of influence attenuation.

In Jefferson High, decay rates for non-smoking spillover rise steadily with coverage, indicating that influence becomes increasingly localized to immediate peers as interventions scale up (Table 1). Under in-degree and eigenvector targeting, decay functions show excellent fit across coverage levels (R^2 = 0.92-0.99 and 0.97-0.99, respectively), with decay rates increasing from 0.267 and 0.284 at 10% coverage to 1.623 and 1.526 by 90%. The strong and stable model fit, especially at lower coverage, suggests that centrality-based strategies not only amplify diffusion but do so in a regular and predictable manner, likely because central individuals facilitate broader and more consistent spillover pathways (5, 6).

<<<<Table 1 about here>>>>

In contrast, random selection yields weaker and less consistent decay patterns, particularly at lower coverage, as reflected in lower R^2 values. Although decay rates under random selection converge with those of centrality-based strategies at higher coverage (e.g., 70%-90%), the instability at lower levels indicates more variable and less effective diffusion when centrality is not prioritized. Overall, these findings affirm that peer influence becomes more short-ranged as networks saturate, reinforcing the diminishing marginal returns discussed previously.

Mirrored patterns emerge for reductions in heavy smoking. Decay functions under in-degree and eigenvector targeting show strong explanatory power (R^2 often > 0.99), with decay rates increasing from around 0.3 at 10% coverage to 1.675 and 1.561 at 90%, respectively. Random selection shows a similar trend but with weaker model fits at lower coverage. Across all strategies, decay rates exceed 1.0 beyond 50% coverage, indicating increasing localized influence as networks approach saturation.

In Sunshine High, where the network is larger and smoking prevalence is lower, patterns are more variable (Table 2). Under random targeting, decay estimates are unstable at low coverage, e.g., 0.805 at 10% but 0.048 at 20% (R^2 = 0.014), indicating weak diffusion; from 30% to 90%, decay rates range from 0.2 to 0.4 with modest fit. In contrast, in-degree targeting shows more consistent increases in decay rates (0.336 to 0.564), and improving model fit, while

eigenvector targeting is the most stable, with decay rates around 0.5-0.6 and R^2 values above 0.9, indicating clearer diffusion when highly connected students are prioritized.

<<<<Table 2 about here>>>>

In Sunshine High, decay patterns for reductions in heavy smoking are more stable than those for non-smoking. At 10%, decay under random selection is immeasurable due to zero-value outcomes, but in-degree and eigenvector targeting yield decay rates of 1.242 and 0.238, respectively, with stronger fit under eigenvector targeting ($R^2 = 0.979$). From 20% onward, decay rates stabilized across strategies, with eigenvector-based targeting producing the highest rates and stronger model fit ($R^2 \approx 0.95$ or higher).

To assess the consequences for interventions that instead target light or moderate smokers, we also estimate decay functions in these instances. As shown in Tables S9-S10, decay estimates are somewhat more variable than those for heavy smokers. Nonetheless, it is notable that the general decay patterns for light smokers are quite similar to those for heavy smokers, with slightly weaker decay slopes. Furthermore, their NAPI curves exhibit a similar shape as heavy smokers, showing increasing attenuation and diminishing spillover beyond roughly 40-50% coverage (Fig. S12 in Supplemental Material).

In summary, centrality-based targeting enhances peer influence and yields predictable diffusion at low-to-moderate coverage. In Jefferson High, the optimal diffusion occur when targeting remains below 40%-50% of heavy smokers; beyond this point, influence becomes increasingly localized with limited marginal returns. In Sunshine High, centrality-based targeting still improves diffusion, but the larger and sparser network dampens spillover. Notably, targeting 10% of heavy smokers in Sunshine (20 out of 2,178) represents a much smaller network proportion than in Jefferson (27 out of 976), reducing initial reach and weaking diffusion at low coverage, particularly under random selection.

Discussion

This study investigates how behavioral change spreads through adolescent friendship networks by simulating targeted interventions to reduce smoking. Using longitudinal data from two Add Health high schools, Jefferson High and Sunshine High, we assess how intervention coverage and selection strategies (random, in-degree centrality, eigenvector centrality) shape both direct effects and indirect spillover. Central to our analysis is estimating peer influence decay across multiple degrees of separation and its interaction with network structure and intervention design.

Several key findings emerge. First, targeting a small fraction of central individuals produces the strongest effects, both directly among those targeted and indirectly through network spillover. Across both schools, in-degree and eigenvector targeting consistently outperformed random selection, particularly at 10%-30% coverage. By leveraging the structural position of well-connected students, these strategies facilitate broader diffusion of behavioral change, consistent with social contagion and diffusion models (*3, 7, 8*).

However, the advantages of centrality-based targeting diminish once coverage exceeds 40%-50%. At higher levels, behavioral change plateaus and the differences between strategies narrow, reflecting network saturation as fewer untapped connections remain. This pattern aligns with previous research on diffusion ceilings and the limited returns of over-targeting in network interventions (*13, 20*).

Critically, intervention effectiveness and influence decay differ across the two school networks. In Jefferson High, where the network is smaller and denser and smoking prevalence is

higher, peer influence appears to diffuse more broadly. In Sunshine High, which has a larger, more diffuse network and lower baseline smoking prevalence, spillover is more limited, particularly at lower coverage. While these differences are consistent with variation in network structure, they may also reflect differences in smoking prevalence or other contextual factors and should therefore be interpreted cautiously. Overall, the results suggest that intervention performance is sensitive to local network and behavioral contexts, rather than governed by a single structural mechanism.

Estimating influence decay rates offers a quantifiable framework for understanding how far interventions extend through social networks. By modeling the exponential decline of peer effects across one to three degrees of separation, we offer empirical support for predictable attenuation with distance (*2, 14*). The decay parameter (δ) enables direct comparison of interventions and diffusion scale, extending prior observational work that documented influence without formally estimating decay. Notably, network distances at the time of intervention strongly predict diffusion despite subsequent tie turnover, suggesting that stable structural features anchor much of this adolescent behavioral transmission.

Policy Implications and Limitations

From a policy perspective, these findings suggest that targeting structurally central individuals can enhance intervention impact, while indiscriminate scale-up yields diminishing returns. In smaller or more cohesive networks, targeting a limited share of highly central individuals (e.g., 10-30% of heavy smokers) may generate meaningful change. In larger, more diffuse environments, where pathways are sparser and spillover attenuates more rapidly, broader strategies may be needed, combining centrality-based targeting with synergistic school-wide, norm-based, or family and community approaches to reinforce behavioral diffusion. The specification of a scalable decay parameter has critical implications for determining the size and cohesion to optimize intervention in a target population prior to going into the field.

While this study provides valuable insights, several limitations exist. First, smoking behaviors were simplified into an ordinal scale, potentially overlooking more nuanced variations. External factors like family or media influences were not explicitly modeled, despite their potential impact on smoking behaviors. Additionally, this analysis focuses on school-based friendship networks and does not incorporate multilayered networks (e.g., online, family, and institutional) that may also influence dynamics.

In addition, the data come from two saturated Add Health schools, one rural and relatively homogeneous (Midwestern Jefferson High) and one suburban and more racially diverse (Northeastern Sunshine High), surveyed in the mid-1990s, prior to the rise of digital and social media. Because adolescent substance use has since changed substantially, with declining cigarette smoking and rising vaping, this socio-temporal context may limit applicability to contemporary settings. Accordingly, caution is warranted when generalizing to today's schools, other regions or cultural contexts, or modern adolescent networks with different communication patterns, peer dynamics, and substance use environments.

Overall, this study offers actionable insights for designing social network-based interventions. Intervention programs targeting adolescent smoking can be informed by a priori understanding of network structure and from anticipating nonlinear diffusion dynamics as interventions scale. Incorporating these factors allows interventions to optimize their impact and leverage peer influence effectively. Meanwhile, this work raises further questions, such as how influence decay functions across networks with varying levels of connectivity, across multiple

layers of adolescents' social environments (e.g., family or online networks), and across different behaviors and age groups. Addressing these questions would help determine the generality of the decay patterns observed here and extend the utility of network-based interventions beyond adolescent smoking to a broader set of behaviorally mediated public health problems.

References and Notes

1. N. E. Friedkin, *A Structural Theory of Social Influence* (Cambridge University Press, 1998).
2. N. A. Christakis, J. H. Fowler, The spread of obesity in a large social network over 32 years. *N. Engl. J. Med*. **357,** 370–379 (2007).
3. N. E. Friedkin, E. C. Johnsen, *Social Influence Network Theory: A Sociological Examination of Small Group Dynamics* (Cambridge University Press, 2011).
4. N. A. Christakis, J. H. Fowler, The spread of obesity in a large social network over 32 years. *N. Engl. J. Med*. **357,** 370–379 (2007).
5. S. E. Asch, Opinions and social pressure. *Sci. Am.* **193,** 31–35 (1955).
6. B. B. Brown, D. R. Clasen, S. A. Eicher, Perceptions of peer pressure, peer conformity dispositions, and self-reported behavior among adolescents. *Dev. Psychol.* **22,** 521–530 (1986).
7. T. W. Valente, Network interventions. *Science* **337,** 49–53 (2012).
8. D. Centola, *How Behavior Spreads: The Science of Complex Contagions* (Princeton University Press, 2018).
9. D. A. Shoham, L. Tong, P. J. Lamberson, A. H. Auchincloss, J. Zhang, L. Dugas, J. S. Kaufman, R. S. Cooper, A. Luke, An actor-based model of social network influence on adolescent body size, screen time, and playing sports. *PLoS ONE* **7,** e39795 (2012).
10. S. C. Montgomery, M. Donnelly, P. Bhatnagar, A. Carlin, F. Kee, R. F. Hunter, Peer social network processes and adolescent health behaviors: A systematic review. *Prev. Med.* **130,** 105900 (2020).
11. C. Wang, O. Lizardo, D. S. Hachen, Using Fitbit data to examine factors that affect daily activity levels of college students. *PLoS ONE* **16,** e0244747 (2021).
12. R. M. Bond, C. J. Fariss, J. J. Jones, A. D. Kramer, C. Marlow, J. E. Settle, J. H. Fowler, A 61-million-person experiment in social influence and political mobilization. *Nature* **489,** 295–298 (2012).
13. E. L. Paluck, H. Shepherd, P. M. Aronow, Changing climates of conflict: A social network experiment in 56 schools. *Proc. Natl. Acad. Sci.* **113,** 566–571 (2016).
14. N. A. Christakis, J. H. Fowler, The collective dynamics of smoking in a large social network. *N. Engl. J. Med.* **358,** 2249–2258 (2008).
15. K. M. Harris, C. T. Halpern, E. A. Whitsel, J. M. Hussey, L. A. Killeya-Jones, J. Tabor, S. C. Dean, Cohort profile: The national longitudinal study of adolescent to adult health (Add Health). *Int. J. Epidemiol.* **48,** 1415–1415k (2019).
16. T. A. B. Snijders, G. G. Van de Bunt, C. E. G. Steglich, Introduction to stochastic actor-based models for network dynamics. *Soc. Netw.* **32,** 44–60 (2010).

17. C. E. G. Steglich, T. A. B. Snijders, M. Pearson, Dynamic networks and behavior: Separating selection from influence. *Sociol. Methodol.* **40,** 329–393 (2010).

18. C. M. Lakon, C. Wang, J. R. Hipp, C. T. Butts, Simulating social network-based interventions for adolescent cigarette smoking. *Soc. Sci. Med.* **380,** 118196 (2025).

19. P. S. Bearman, J. Moody, K. Stovel, Chains of affection: The structure of adolescent romantic and sexual networks. *Am. J. Sociol.* **110,** 44–91 (2004).

20. D. R. Hunter, P. N. Krivitsky, M. S. Handcock, Computational statistical methods for social network models. *J. Comput. Graph. Stat.* **28,** 830–841 (2019).

Acknowledgments:

Funding: U.S. National Institutes of Health (NIH) Grant #1 R21 DA031152-01A1.

Author contributions:

Conceptualization: C.W., C.T.B., J.R.H., and C.M.L.

Methodology: C.W.

Formal analysis: C.W., C.T.B.

Investigation: C.W.

Visualization: C.W., C.T.B.

Funding acquisition: C.M.L.

Project administration: C.M.L.

Supervision: C.M.L.

Writing – original draft: C.W., C.T.B., J.R.H., and C.M.L.

Writing – review & editing: C.W., C.T.B., J.R.H., and C.M.L.

Competing interests: Authors declare that they have no competing interests.

Data and materials availability: Information on how to obtain the Add Health data files is available on the Add Health website (http://www.cpc.unc.edu/addhealth).

Supplemental Materials

Materials and Methods

Figs. S1 to S12

Tables S1 to S10

A

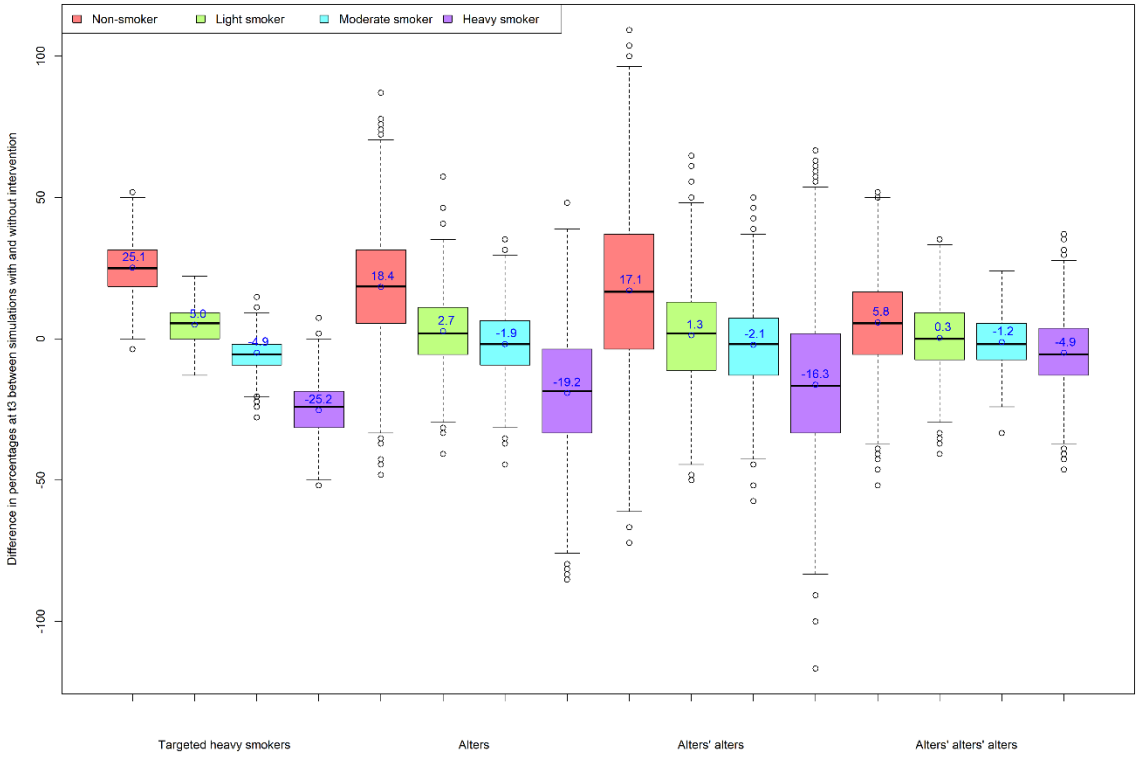
Non-smoker
Light smoker
Moderate smoker
Heavy smoker
Difference in percentages at t3 between simulations with and without intervention
100
50
0
-50
-100
25.1
5.0
-4.9
-25.2
18.4
2.7
-1.9
-19.2
17.1
1.3
-2.1
-16.3
5.8
0.3
-1.2
-4.9
Targeted heavy smokers
Alters
Alters' alters
Alters' alters' alters

B

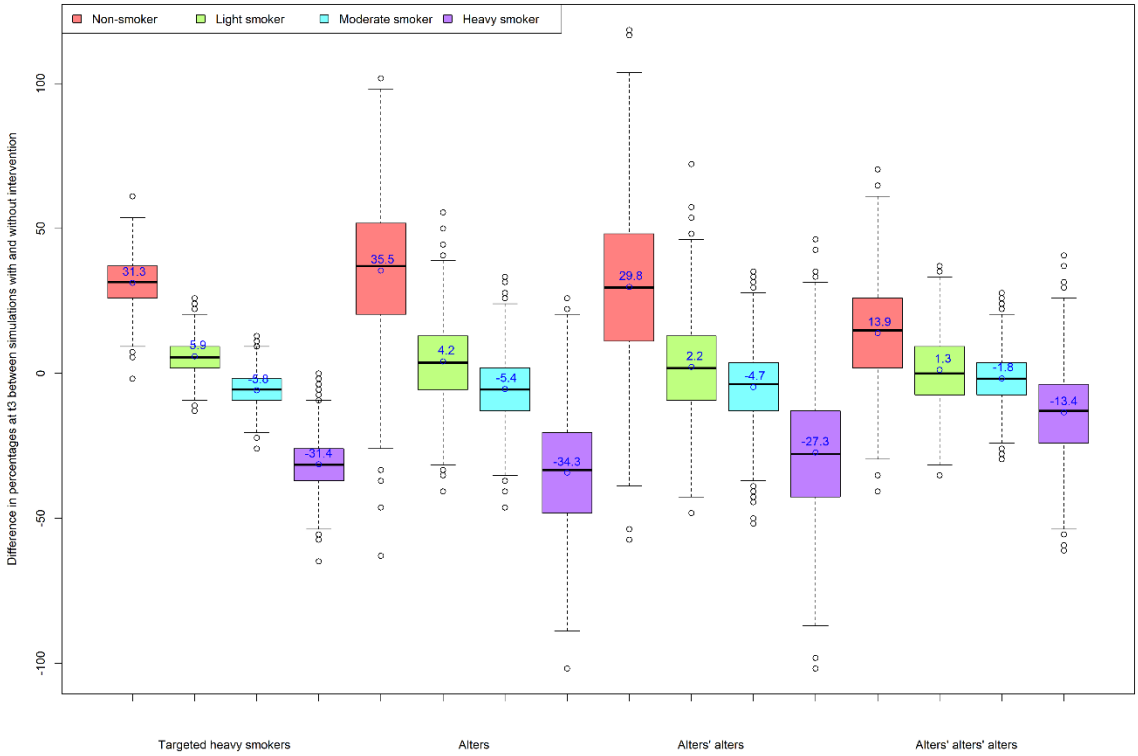
Non-smoker
Light smoker
Moderate smoker
Heavy smoker
Difference in percentages at t3 between simulations with and without intervention
100
50
0
-50
-100
31.3
5.9
-5.8
-31.4
35.5
4.2
-5.4
-34.3
29.8
2.2
-4.7
-27.3
13.9
1.3
-1.8
-13.4
Targeted heavy smokers
Alters
Alters' alters
Alters' alters' alters

C

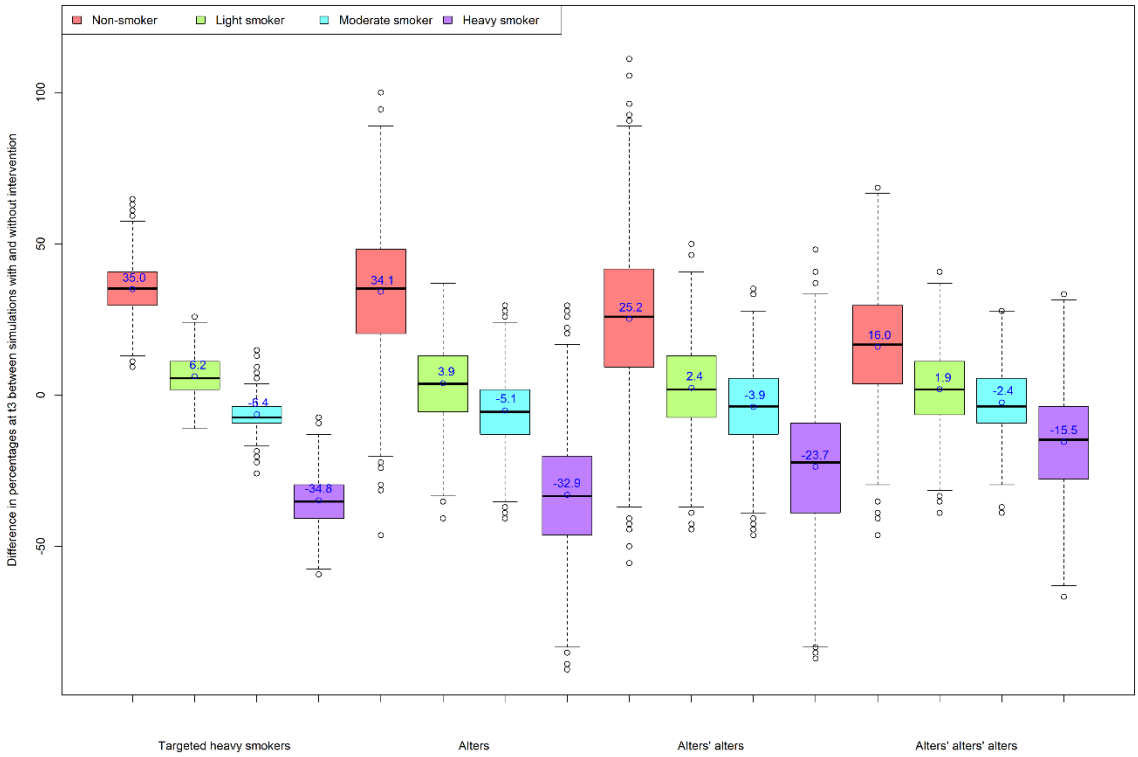

Fig. 1. Effects of targeting 20% of heavy smokers in Jefferson High (n = 976), disaggregated by targeting strategy and social distance. (A) Random selection. **(B)** In-degree centrality. **(C)** Eigenvector centrality. Each panel shows changes in smoking status (non-smoker, light, moderate, heavy) at wave t_3 among targeted individuals and their peers up to three degrees away (first-, second-, and third-degree alters), based on comparisons between intervention and control simulations.

A

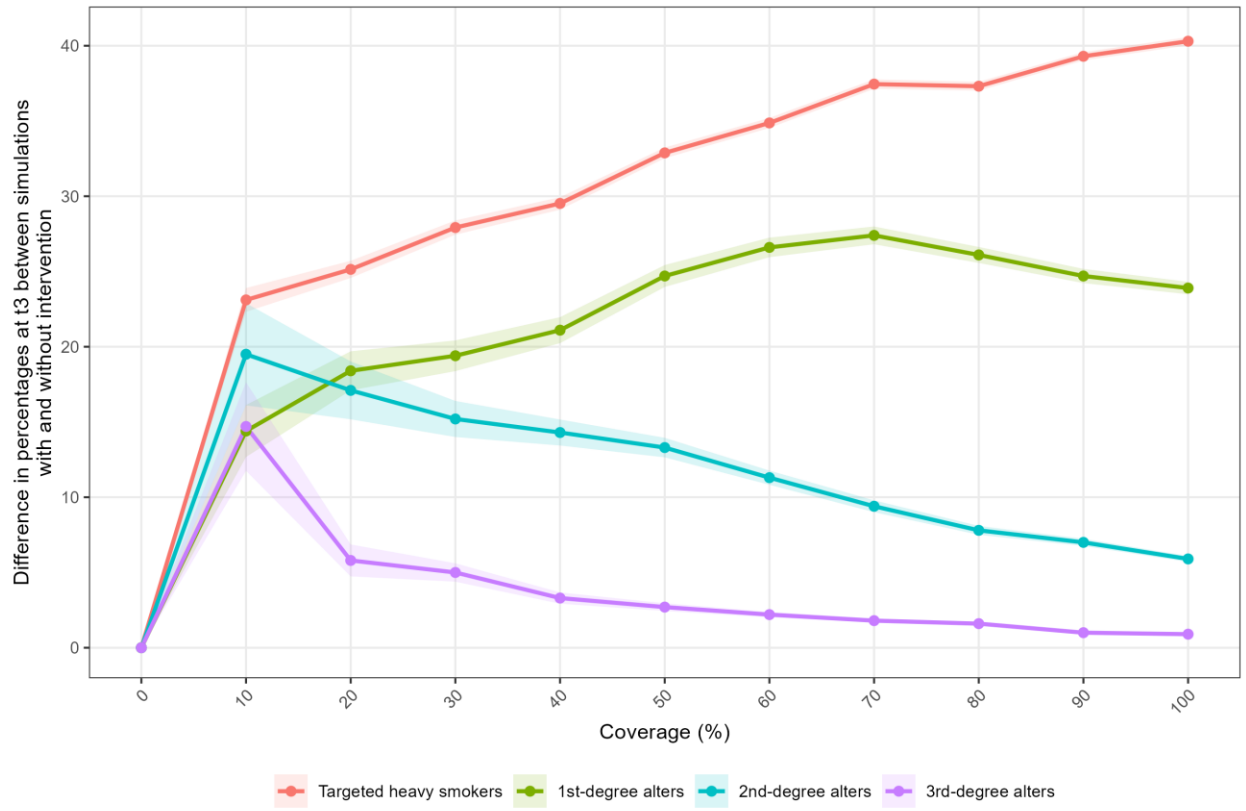
Difference in percentages at t3 between simulations with and without intervention
0
10
20
30
40
0
10
20
30
40
50
60
70
80
90
100
Coverage (%)
Targeted heavy smokers
1st-degree alters
2nd-degree alters
3rd-degree alters

B

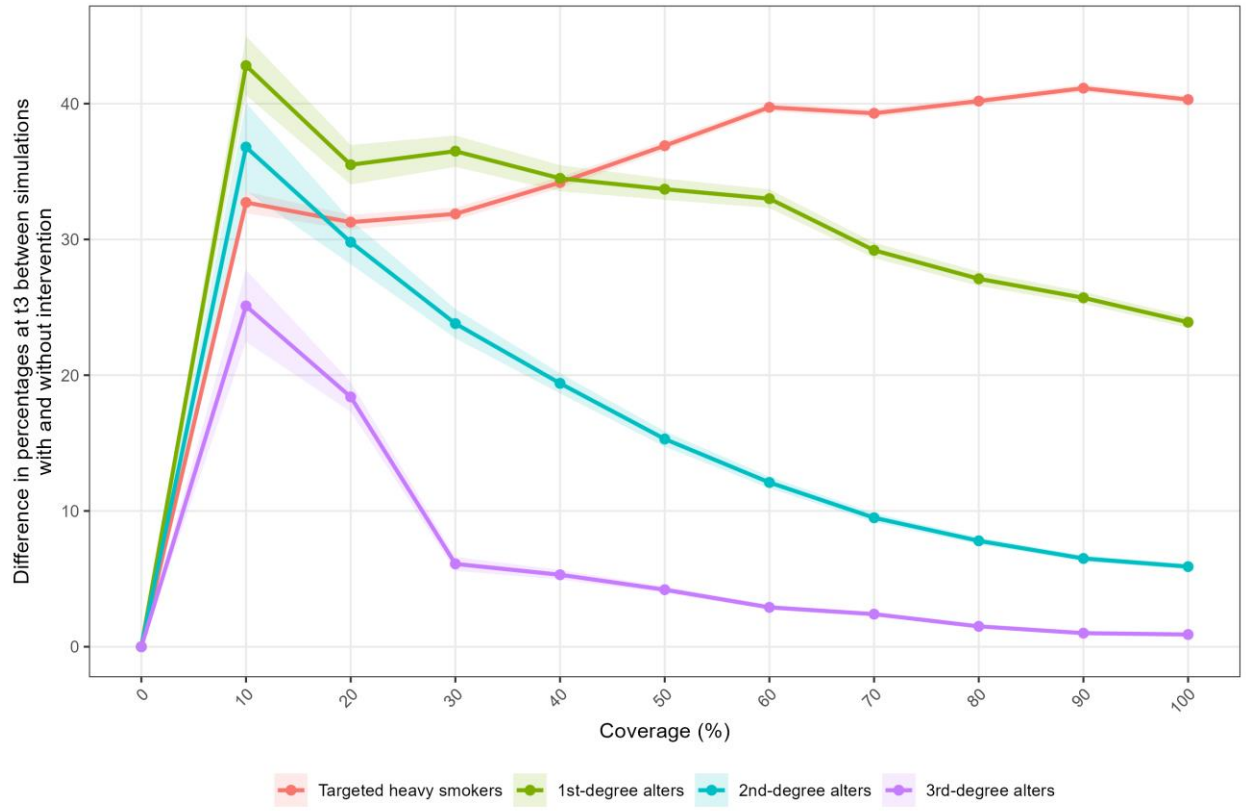
Difference in percentages at t3 between simulations with and without intervention
0
10
20
30
40
0
10
20
30
40
50
60
70
80
90
100
Coverage (%)
Targeted heavy smokers
1st-degree alters
2nd-degree alters
3rd-degree alters

C

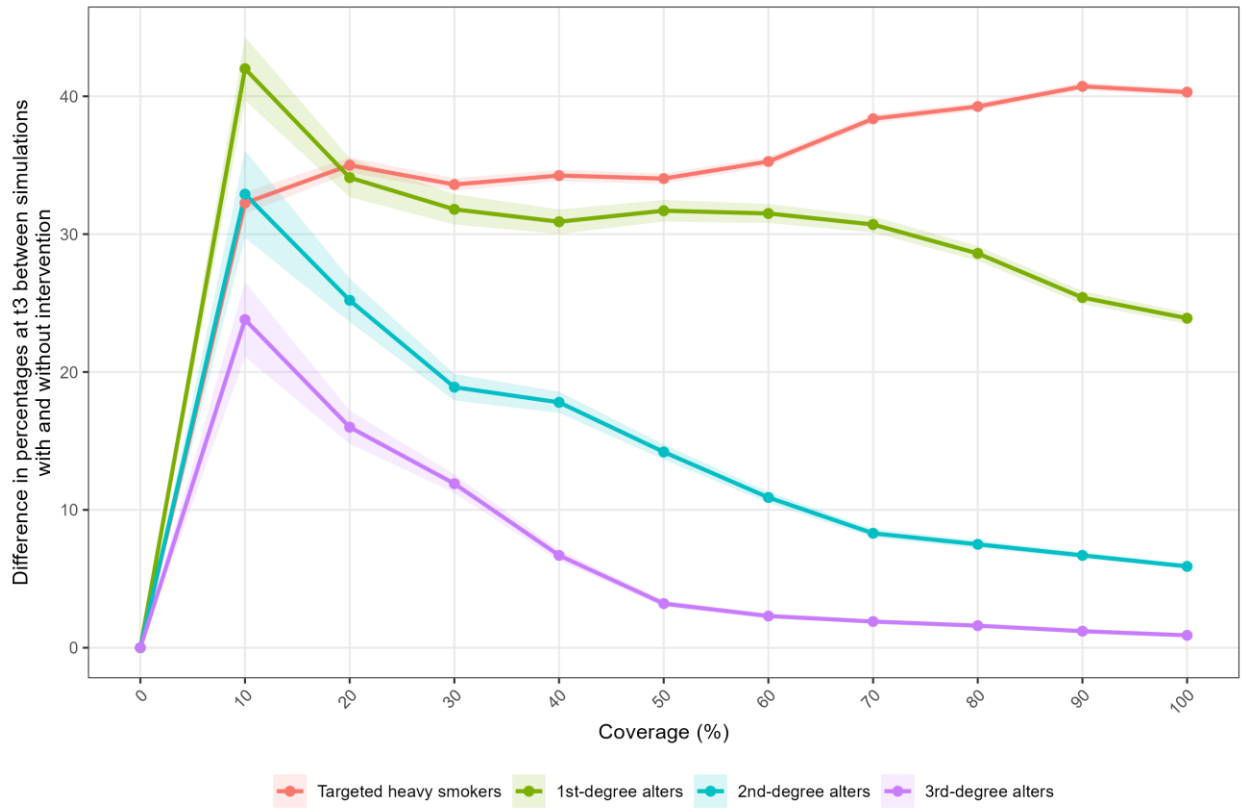

Fig. 2. Intervention outcomes by targeting strategy and coverage on non-smoking in Jefferson High (n = 976). **(A)** Random selection. **(B)** In-degree centrality. **(C)** Eigenvector centrality. Each panel displays changes in non-smoking rates at t_3 across four social distances: targeted heavy smokers, their first-, second, and third-degree alters. Shaded bands indicate 95% confidence intervals. Results are based on simulated interventions targeting 10%-100% of heavy smokers.

Table 1. Decay rates/R^2 of peer influence from targeted students on non-smoking and heavy smoking across selection proportions and targeting strategies in Jefferson High (n = 976).

Selection Proportion (%)	random / non-smoker	in-degree / non-smoker	eigenvector / non-smoker	random / heavy smoker	in-degree / heavy smoker	eigenvector / heavy smoker
10%	-0.010/0.004	0.267/0.941	0.284/0.993	0.077/0.310	0.299/0.966	0.265/1.000
20%	0.577/0.797	0.329/0.932	0.378/0.987	0.683/0.838	0.345/0.963	0.376/0.995
30%	0.678/0.880	0.895/0.917	0.491/0.999	0.752/0.906	0.948/0.919	0.494/1.000
40%	0.928/0.899	0.937/0.953	0.764/0.975	1.003/0.919	1.000/0.954	0.738/0.986
50%	1.107/0.939	1.041/0.981	1.147/0.971	1.168/0.955	1.066/0.985	1.150/0.976
60%	1.246/0.968	1.216/0.990	1.309/0.988	1.323/0.976	1.229/0.996	1.334/0.988
70%	1.361/0.985	1.249/0.997	1.391/0.999	1.451/0.988	1.271/0.998	1.401/1.000
80%	1.396/0.994	1.447/0.994	1.442/0.998	1.496/0.994	1.468/0.998	1.490/1.000
90%	1.603/0.985	1.623/0.992	1.526/0.995	1.666/0.992	1.675/0.996	1.561/0.998
100%	1.640/0.993			1.708/0.996		

Table 2. Decay rates/R^2 of peer influence from targeted students on non-smoking and heavy smoking across selection proportions and targeting strategies in Sunshine High (n = 2,178).

Selection Proportion (%)	random / non-smoker	in-degree / non-smoker	eigenvector / non-smoker	random / heavy smoker	in-degree / heavy smoker	eigenvector / heavy smoker
10%	0.805/0.464	1.070/0.462	0.781/0.807	-	1.242/0.470	0.238/0.979
20%	0.048/0.014	0.525/0.901	0.596/0.902	0.458/0.499	0.766/0.967	1.040/0.970
30%	0.221/0.970	0.336/0.882	0.618/1.000	0.131/0.111	0.452/0.965	0.945/0.966
40%	-0.027/0.095	0.440/0.670	0.427/0.855	0.288/0.672	0.527/0.908	0.606/0.996
50%	0.235/0.642	0.549/0.995	0.503/0.710	0.321/0.941	0.723/0.987	0.650/0.933
60%	0.263/0.529	0.523/0.927	0.515/0.962	0.347/0.750	0.534/0.971	0.549/0.957
70%	0.290/0.561	0.525/0.883	0.525/0.994	0.321/0.859	0.665/0.982	0.709/0.993
80%	0.249/0.487	0.564/0.995	0.509/0.931	0.347/0.657	0.711/1.000	0.677/0.998
90%	0.314/0.521	0.444/0.969	0.535/0.961	0.458/0.827	0.585/0.995	0.644/0.994
100%	0.413/0.994			0.540/0.989		